

## Effect of one-step and two-step homogenization treatments on distribution of $\text{Al}_3\text{Zr}$ dispersoids in commercial AA7150 aluminium alloy

LÜ Xin-yu<sup>1,2</sup>, GUO Er-jun<sup>1</sup>, Paul ROMETSCH<sup>3</sup>, WANG Li-juan<sup>2</sup>

1. School of Materials Science and Engineering, Harbin University of Science and Technology,  
Harbin 150080, China;  
2. Northeast Light Alloy Co Ltd., Harbin 150060, China;  
3. ARC Centre of Excellence for Design in Light Metals, Department of Materials Engineering,  
Monash University, Melbourne VIC 3800, Australia

Received 21 March 2012; accepted 14 September 2012

**Abstract:** Semi-quantitative electron probe microanalysis (EPMA) mapping, scanning electron microscopy (SEM) and transmission electron microscopy (TEM) were employed to study the effect of one-step and two-step treatments on the Zr distribution and  $\text{Al}_3\text{Zr}$  dispersoid characteristics in as-cast commercial AA7150 aluminium alloy. It is shown that the Zr concentration in the dendrite centre regions is higher than that near the dendrite edges in the as-cast condition, and that homogenization at 460 °C for 20 h is insufficient to remove these concentration gradients. After homogenizing at 460–480 °C, a high number density of larger dispersoids can be observed in dendrite centre regions but not near dendrite edges. Furthermore, the dispersoid size increases with increasing the temperature during both one-step and two-step homogenization treatments.

**Key words:** 7xxx alloy; AA7150 alloy; homogenization; recrystallization;  $\text{Al}_3\text{Zr}$  dispersoids; concentration gradient

### 1 Introduction

Commercial AA7150 aluminium alloy is widely used as an airplane upper wing structural material due to its excellent balance of properties, such as strength, toughness and stress corrosion cracking resistance [1–3].

Small addition of zirconium can improve the properties of high strength of wrought aluminium alloys by forming metastable and coherent  $\text{Al}_3\text{Zr}$  dispersoids, which inhibit recrystallization by means of a grain boundary pinning mechanism [4]. It has been shown that the inhomogeneous distribution of dispersoid particles leads to a lower resistance to recrystallization in the regions adjacent to grain boundaries, and that large primary  $\text{Al}_3\text{Zr}$  particles can even promote recrystallization [5–8]. The effectiveness of the dispersoids for controlling recrystallization depends on their size, spacing and distribution, which are strongly influenced by the homogenization treatment [9]. In practice, homogenization is usually used to dissolve the maximum volume of unwanted eutectic phases and

redistribute the solute [10], rather than to optimize dispersoid precipitation. However, it is possible to increase the effectiveness of the dispersoids by tuning the homogenization conditions and zirconium concentration [11]. To get the best distribution of dispersoids, some uses a novel process model to optimize the homogenization of zirconium containing commercial aluminium alloy [12], and some researches the segregation in  $\text{Al}_3(\text{Sc},\text{Zr})$  precipitates in Al–Sc–Zr alloy[13]. But few put emphasis on the effect of one-step and two-step homogenization treatments.

The purpose of this work is: 1) to study the effect of homogenization on the concentration profiles of Zr across dendrites and to observe whether or not the as-cast concentration gradients could be removed by homogenization; 2) to investigate the homogenization temperature required to generate an optimized dispersoid distribution; and 3) to determine whether a two-step homogenization treatment can lead to an improved dispersoid distribution that could decrease the fraction of recrystallization compared with a conventional single-step treatment.

## 2 Experimental

### 2.1 Materials

The samples used in this study were obtained from a large industrial direct chill cast 7150 ingot with a chemical composition of Al–6.6Zn–2.3Mg–2.2Cu–0.12Zr–0.07Fe–0.02Si (mass fraction, %).

### 2.2 Homogenization treatments

Two types of homogenization treatments were used in this study. The first one was a single-step homogenization treatment, where samples were held for 20 h at 400, 430, 460 and 480 °C, respectively. The second one was a two-step homogenization treatment with two different processes. In the first case, the sample was homogenized at 400 °C for 20 h, and then slowly heated to 460 °C and held for 10 h. In the other case, the sample was homogenized at 430 °C for 20 h, and then slowly heated to 470 °C and held for 10 h. After the homogenization treatment, the samples were quenched in room temperature water.

### 2.3 Microstructure analysis

The as-cast and homogenized samples were polished and mounted for microstructural analysis on a JEOL JSM 7001F FEG scanning electron microscope (SEM). Semi-quantitative electron probe microanalysis (EPMA) with wavelength dispersive spectroscopy (WDS) was used to determine the concentrations of various elements across dendrites in the as-cast and homogenized conditions. For each dendrite, the microprobe scans were carried out at 8 kV with a step size of 200 nm and along 20 parallel lines that were 500 nm apart. As a result, each scan covered an area of about 10 μm × 120 μm (approximately 12000 points) and took about 30 min each to complete.

## 3 Results and discussion

### 3.1 Electron probe microanalysis

Figure 1 shows the electron probe microanalysis (EPMA) mapping results, with relative Zr concentration plotted across representative dendrites in the as-cast and homogenized conditions. Mapping was performed across the dendrites shown in the associated backscattered electron images. In some cases, such as in Fig. 1(c), the scans may have crossed more than one dendrite since the boundaries were not always visible (i.e. they have been below the surface). It is evident that in the as-cast condition, the Zr concentration in the dendrite centre regions is higher than that near the dendrite edges. This is due to a typical peritectic solidification reaction associated with Zr, which results in Zr-rich regions at the

cores of the dendrites.

After homogenizing at 400 °C for 20 h, the Zr concentration profile across the dendrites appears to be similar to that in the as-cast condition, suggesting that no significant diffusion of Zr has occurred. After homogenizing at 460 °C for 20 h, the Zr concentration is still inhomogeneous, indicating that the diffusion rate of Zr is extremely low in aluminium at these temperatures. If any Al<sub>3</sub>Zr precipitation appears, it can be expected to be a very localized event.

In order to confirm these findings, a set of higher resolution EPMA scans were performed. Figure 2 shows the relative concentration of Zr across a dendrite in the sample that was homogenized at 460 °C for 20 h. The grey map shows atomic number contrast, while the others are color coded as indicated. Both the atom map and the graphs of the Zr distribution show regions of high Zr concentration around the dendrite centre and low Zr concentration near the dendrite edge. This confirms the results from the homogenization treatment at 460°C in Fig. 1(c), namely, the Zr concentration profile has not been homogenized by this treatment.

### 3.2 Backscattered SEM images after single-step homogenization

The backscattered scanning electron microscopy (SEM) images in Fig. 3 show the distribution of Al<sub>3</sub>Zr dispersoids in different locations across dendrites in the differently heat-treated samples. It can be seen that spherical Al<sub>3</sub>Zr dispersoids are very difficult to be found and resolved by SEM in the as-cast condition and after homogenizing at 400 °C. However, after one-step homogenizing at either 460 °C or 480 °C for 20 h, Al<sub>3</sub>Zr dispersoids can be easily resolved as white dots on the backscattered SEM images due to the high atomic number of Zr. The EDS analyses in Fig. 4 and Table 1 show that those white dots contain a significant amount of Zr, suggesting that they are Al<sub>3</sub>Zr dispersoids rather than Zn- or Fe-based phases [14]. The fact that these white dots are observed much more around the dendrite centre regions than at the dendrite edges confirms the EPMA findings that these homogenization treatments are not sufficient to remove the Zr concentration gradients. By contrast, the EPMA results indicate that the as-cast concentration gradients due to Zn, Mg and Cu (i.e. coring) are already completely removed after 20 h at 400 °C. It should be noted that the elongated particles in the as-cast condition in Fig. 3 are MgZn<sub>2</sub> precipitates.

### 3.3 TEM microstructures

Transmission electron microscopy (TEM) was employed to confirm that the spherical white dispersoids in Fig. 3 are metastable Al<sub>3</sub>Zr as shown in Fig. 5. Equilibrium Al<sub>3</sub>Zr dispersoids were not detected in any

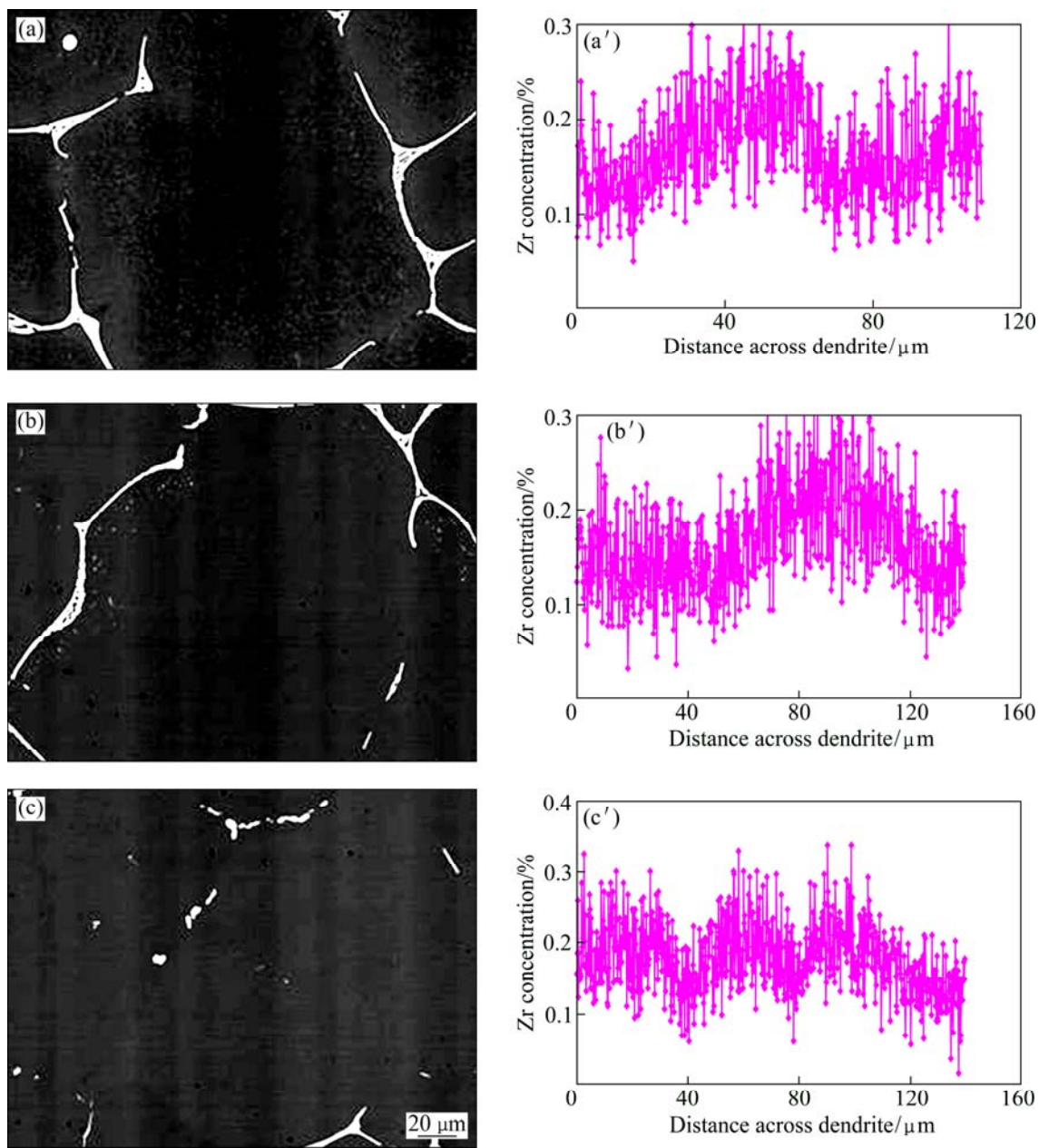


**Fig. 1** Electron probe microanalysis (EPMA) mapping results for AA7150 alloy in following states: (a,a') As-cast; (b,b') homogenized at 400 °C for 20 h; (c, c') homogenized at 460 °C for 20 h

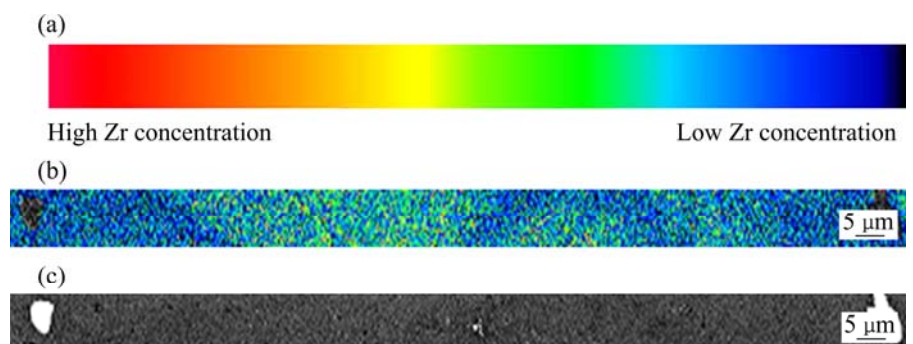


**Fig. 2** High resolution EPMA maps AA7150 alloy showing relative concentration of Zr across a dendrite after homogenization at 460 °C for 20 h: (a) Zr atom map; (b) Zr distribution map; (c) Back scattered electron image

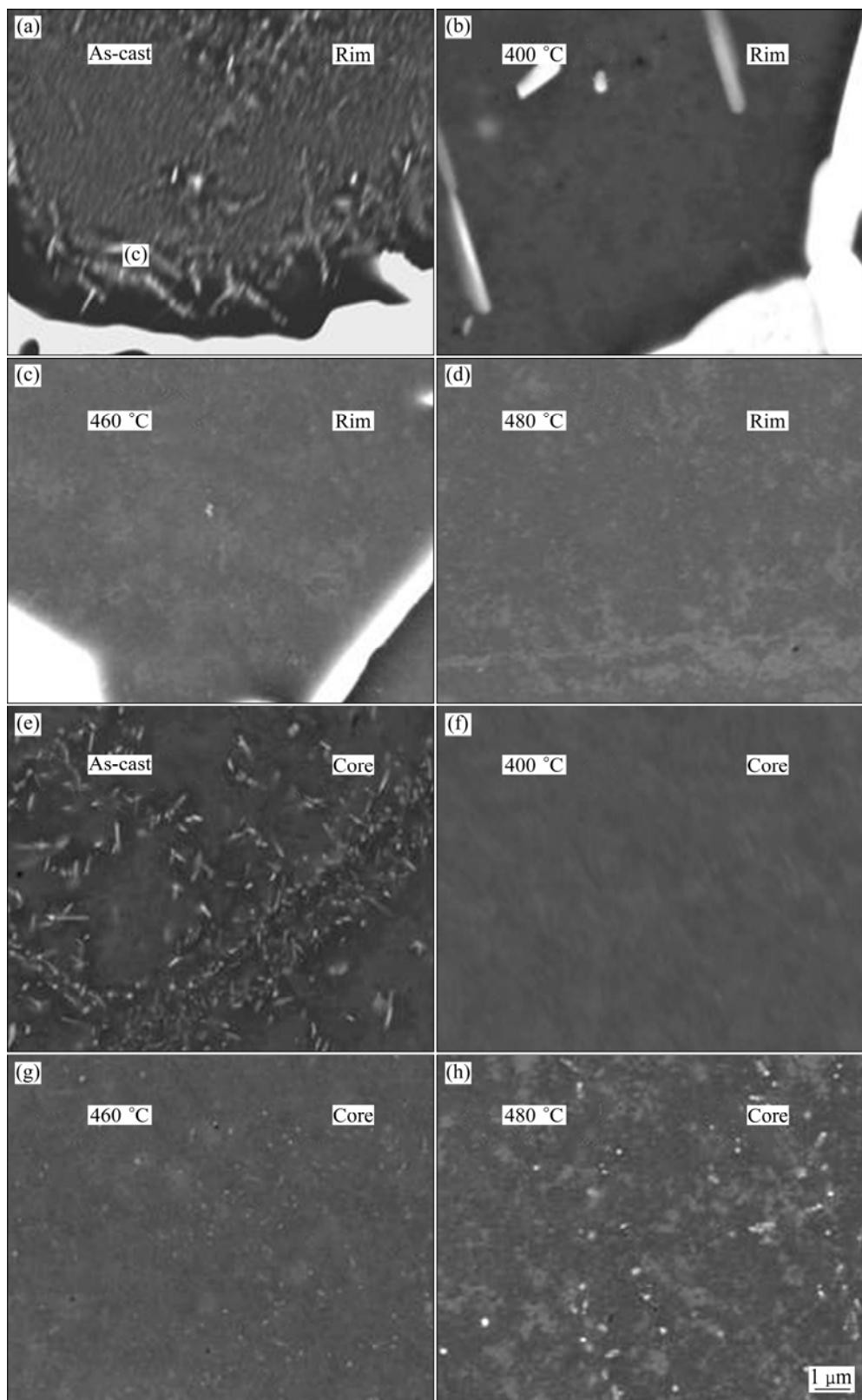


**Fig. 3** Backscattered SEM images taken at dendrite rim (a,b,c,d) and core (e,f,g,h) locations in as-cast condition (a,e) and after 20 h at indicated homogenization temperatures of 400 °C (b,f), 460 °C (c,g), 480 °C (d,h)

of the conditions examined in this work. TEM images in Fig. 5 show that a relatively high number density of  $\text{Al}_3\text{Zr}$  dispersoids (approximately 20–50 nm in diameter)

can be observed in the samples homogenized at either 460 °C or 480 °C for 20 h. However, when the samples were homogenized between 400 and 430 °C,  $\text{Al}_3\text{Zr}$

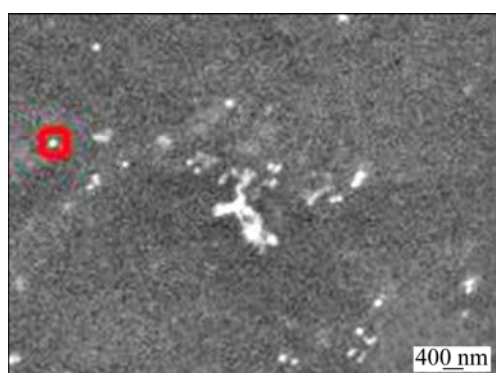


**Fig. 4** Higher magnification backscattered electron image

**Table 1** Energy dispersive spectrometer (EDS) results for small white dots in highlighted area taken from sample homogenized for 20 h at 460 °C in Fig. 4

Element	Series	w/%	x/%	Error in mass fraction/%
Magnesium	K-series	1.5	1.8	0.1
Aluminium	K-series	84.5	92.2	3.0
Copper	K-series	3.0	1.4	0.5
Zinc	K-series	8.4	3.8	0.9
Zirconium	L-series	2.5	0.8	0.2
Sum		100	100	

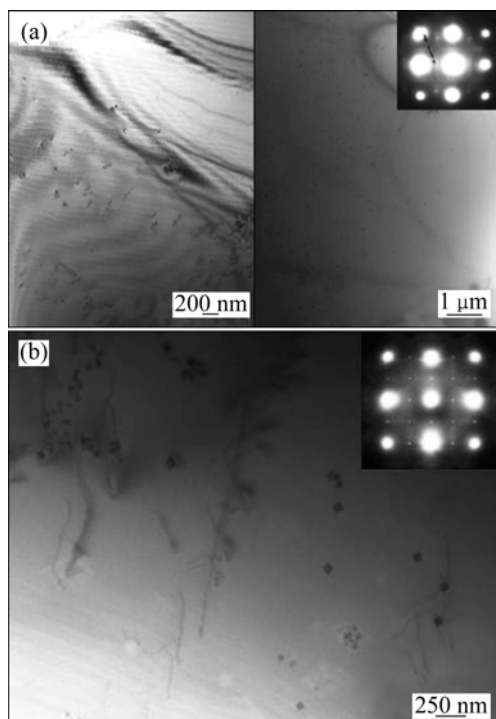


**Fig. 5** TEM images showing  $\text{Al}_3\text{Zr}$  dispersoids after homogenizing for 20 h at 460 °C (a), and 480 °C (b)

dispersoids could not be observed, as shown in Fig. 6. However, it should be noted that the limitation of TEM is that the examined area is very small compared to the

scale of the non-uniform distribution of the dispersoids throughout the samples. Based on a combination of both the TEM and SEM results, it can be concluded that homogenization at 400–430 °C results in either very few or very small dispersoids, while homogenization above about 450 °C results in a higher number density of larger dispersoids that can be easily detected by SEM, namely, their size also appears to increase at the higher temperatures.

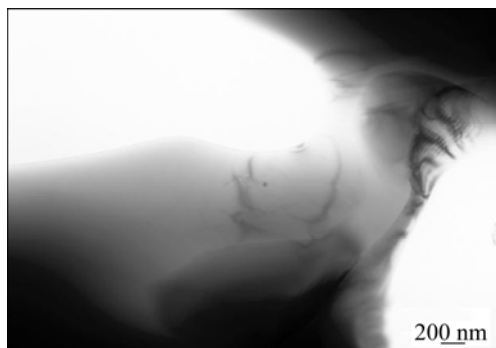


**Fig. 6** Typical TEM image after homogenizing for 20 h at 400–430 °C

It was reported [15] that the nucleation rate for the formation of  $\text{Al}_3\text{Zr}$  dispersoids is dependent on the Zr concentration and the temperature. The maximum nucleation rate increases with increasing Zr concentration, and the temperature for the maximum nucleation rate shifts to higher temperatures with higher Zr concentration. Furthermore, the rate for the growth of  $\text{Al}_3\text{Zr}$  dispersoids has a similar trend as the relationship between nucleation rate on Zr concentration and temperature. It is suggested that at a certain Zr concentration, a high homogenization temperature is required to obtain a maximum nucleation and growth rate. In the case of this study, with 0.12% Zr, the results suggest that a homogenization temperature higher than 450 °C is required to promote a rapid precipitation and growth of dispersoids. Therefore, homogenization at 400–430 °C results in either very few or very small dispersoids, while homogenization above about 450 °C results in a higher number density of larger dispersoids.

### 3.4 Effect of two-step homogenization treatments

The heterogeneous distribution of zirconium during solidification causes the zirconium concentration towards the edges of dendrites to be insufficient to precipitate dispersoids. As a result, dispersoid-free zones are formed in the interdendritic regions close to the original grain boundaries. In addition, the large particles along the grain boundaries can easily stimulate the nucleation of recrystallized grains during solution treatment. Therefore, the number of dispersoids near the edges of dendrites

plays a critical role in controlling recrystallization. It can prevent the growth of recrystallized grains if there is sufficient Zener drag [16,17]:

$$p_z = \frac{3V_f \gamma}{r} \quad (1)$$

where  $V_f$  is the local volume fraction of the dispersoids;  $r$  is the particle radius;  $\gamma$  is the energy of the boundary that the dispersoids are pinned. It can be seen from this equation that the Zener drag due to the dispersoids is maximized by maximizing the volume fraction ( $V_f$ ) and minimizing the particle size. As a result, the reason for low zirconium regions causing recrystallization is that the  $V_f/r$  ratio is too low. Therefore it is necessary to increase the  $V_f/r$  ratio by optimizing the homogenization treatment. However, none of the single-step homogenization treatments in this work was able to achieve a modified distribution of zirconium dispersoids with a high  $V_f/r$  ratio, since a low one-step homogenization temperature leads to low nucleation and growth rates, while a high one-step homogenization temperature may result in a low nucleation rate and a

high growth rate. Therefore, a modified homogenization treatment (i.e. two-step homogenization) is needed to promote the nucleation of the dispersoids while prevent too much growth of the dispersoids.

Although the homogenization can not completely remove the Zr concentration gradients from the as-cast alloy, two-step homogenization treatment can result in a more uniform  $\text{Al}_3\text{Zr}$  dispersoid distribution than that achieved by one-step homogenization treatment. In the two-step homogenization treatment, the first step should be carried out at a relatively low temperature to promote the nucleation of dispersoids, and a higher temperature should be employed in the second step treatment in order to promote the controlled growth of the dispersoids.

Figure 7 shows the backscattered SEM images after two-step homogenization treatment of  $400\text{ }^\circ\text{C}+460\text{ }^\circ\text{C}$  (top) and  $430\text{ }^\circ\text{C}+470\text{ }^\circ\text{C}$  (bottom), which were taken at the dendrite rim, quarter and core locations. More and larger  $\text{Al}_3\text{Zr}$  dispersoids are observed around the dendrite centres than around the dendrite edges. These results correlate well with the EPMA results, which show a higher concentration of Zr near the dendrite centres.

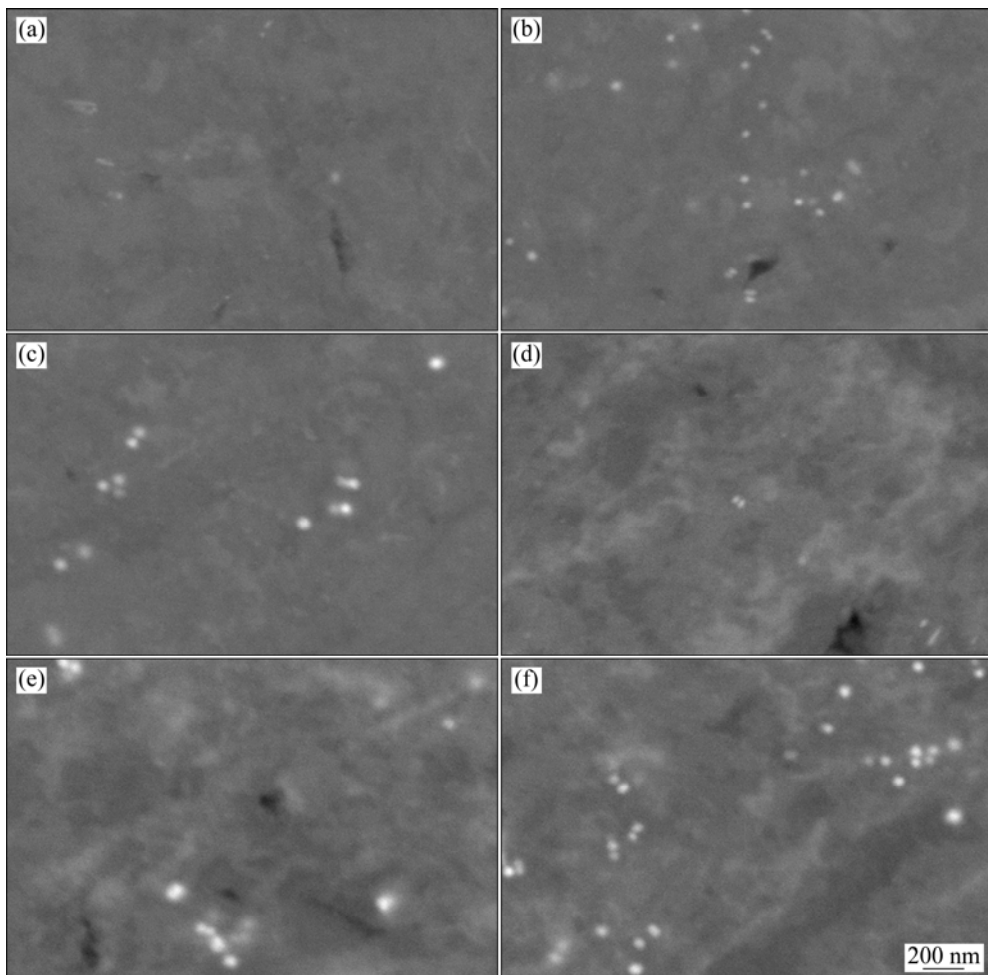


**Fig. 7** Backscattered SEM images taken at dendrite rim (a,d), quarter (b,e) and core (c,f) locations after two-step homogenization treatments at  $400\text{ }^\circ\text{C}+460\text{ }^\circ\text{C}$  (a,b,c), and  $430\text{ }^\circ\text{C}+470\text{ }^\circ\text{C}$  (d,e,f)

Furthermore, the 430 °C + 470 °C treatment results in coarser dispersoids than the 400 °C + 460 °C homogenization treatment.

## 4 Conclusions

1) In the as-cast condition, the Zr concentration in the dendrite centre regions is higher than that near the dendrite edges. Homogenizing for 20 h at 460 °C is not sufficient to remove this Zr concentration gradient.

2) Homogenization at 400–430 °C results in either very few or very small dispersoids, while homogenization above 450 °C promotes the formation of a higher number of larger dispersoids.

3) Dispersoids formed during homogenization are concentrated around dendrite centre regions and increase in size with increasing temperature.

## Acknowledgements

The authors thank Sam Gao at Monash University for the TEM results and Colin MacRae at CSIRO Process Science and Engineering for the EPMA results. Use of the facilities at the Monash Centre for Electron Microscopy (MCEM) is also gratefully acknowledged.

## References

- [1] SRIVATSAN T S, ANAND S, SRIRAM S, VASUDEVAN V K. The high-cycle fatigue and fracture behavior of aluminum alloy 7055 [J]. Materials Science and Engineering A, 2000, 281: 292–304.
- [2] CHRISTIAN J W. The theory of transformations in metals and alloys [M]. Pergamon: Oxford, 1965.
- [3] LIU S D, ZHANG X M, CHEN M A, YOU J H. Influence of aging on quench sensitivity effect of 7055 aluminum alloy [J]. Materials Characterization, 2008, 59: 53–60.
- [4] SHA G, CEREZO A. Early-stage precipitation in Al–Zn–Mg–Cu alloy (7050) [J]. Acta Materialia, 2004, 52(15): 4503–4516.
- [5] MONDAL C, MUKHOPADHYAY A K, RAGHU T, VARMA V K. Tensile properties of peak aged 7055 aluminum alloy extrusions [J]. Materials Science and Engineering A, 2007, 454–455: 673–678.
- [6] POURKIA N, EMAMY M, FARHANGI H, SEYED EBRAHIMI S H. The effect of Ti and Zr elements and cooling rate on the microstructure and tensile properties of a new developed super high-strength aluminum alloy [J]. Materials Science and Engineering A, 2010, 527: 5318–5325.
- [7] GHOSH G, ASTA M. First-principles calculation of structural energetics of Al–TM (TM=Ti, Zr, Hf) intermetallics [J]. Acta Materialia, 2005, 53: 3225–3252.
- [8] SHA G, CEREZO A. Field ion microscopy and 3-D atom probe analysis of Al<sub>3</sub>Zr particles in 7050 Al alloy [J]. Ultramicroscopy, 2005, 102: 151–159.
- [9] ROBSON J D. A new model for prediction of dispersoid precipitation in aluminium alloys containing zirconium and scandium [J]. Acta Materialia, 2004, 52: 1409–1421.
- [10] ROBSON J D, PRANGNELL P B. Dispersoid precipitation and process modeling in zirconium containing commercial aluminum alloys [J]. Acta Materialia, 2001, 49: 599–613.
- [11] DESCHAMPS A, LAE L, GUYOT P. In situ small-angle scattering study of the precipitation kinetics in an Al–Zr–Sc alloy [J]. Acta Materialia, 2007, 55: 2775–2783.
- [12] ROBSON J D. Optimizing the homogenization of zirconium containing commercial aluminium alloys using a novel process model [J]. Materials Science and Engineering A, 2002, 338: 219–229.
- [13] TOLLEY A, RADMILOVIC V, DAHMEN U. Segregation in Al<sub>3</sub>(Sc,Zr) precipitates in Al–Sc–Zr alloys [J]. Scripta Materialia, 2005, 52: 621–625.
- [14] WLOKA J, VIRTANEN S. Influence of scandium on the pitting behaviour of Al–Zn–Mg–Cu alloys [J]. Acta Materialia, 2007, 55: 6666–6672.
- [15] ENGLER O. Nucleation and growth during recrystallization of aluminium alloys investigated by local texture analysis [J]. Mater Sci Tech, 1996, 12: 859–872.
- [16] JAZAERI H, HUMPHREYS F J. The transition from discontinuous to continuous recrystallization in some aluminium alloys: II—Annealing behavior [J]. Acta Materialia, 2004, 52: 3251–3262.
- [17] NES E, RYUM N, HUNDERI O. On the Zener drag [J]. Acta Metallurgica, 1985, 33: 11–22.

# 单级及双级均匀化处理工艺对 AA7150 合金 Al<sub>3</sub>Zr 弥散相析出的影响

吕新宇<sup>1,2</sup>, 郭二军<sup>1</sup>, Paul ROMETSCH<sup>3</sup>, 王立娟<sup>2</sup>

1. 哈尔滨理工大学 材料科学与工程学院, 哈尔滨 150080;
2. 东北轻合金有限责任公司, 哈尔滨 150060;
3. ARC Centre of Excellence for Design in Light Metals, Department of Materials Engineering,  
Monash University, Melbourne, VIC 3800, Australia

**摘要:** 用半定量电子探针、扫描电镜、透射电镜方法, 分析了单、双级均匀化对 AA7150 合金中 Al<sub>3</sub>Zr 分布的影响。结果表明, 在铸态条件下 Zr 在枝晶心部浓度高, 枝晶边缘处浓度低。在均匀化温度 460 °C 下处理 20 h 并不足以改变其浓度梯度。当均匀化温度达到 460~480 °C 时, 在枝晶心部可获得大量的 Al<sub>3</sub>Zr 弥散相, 且 Al<sub>3</sub>Zr 弥散相的尺寸随着单双级均匀化处理温度的升高而增大。

**关键词:** 7xxx 合金; AA7150 合金; 均匀化; 再结晶; Al<sub>3</sub>Zr 弥散; 浓度梯度

(Edited by YANG Hua)